# Singular and regular gap solitons between three dispersion curves

Roger Grimshaw*
*Department of Mathematical Sciences, Loughborough University, Loughborough, LE11 3TU, United Kingdom*

Boris A. Malomed†
*Department of Interdisciplinary Studies, Faculty of Engineering, Tel Aviv University, Tel Aviv 69978, Israel*

Georg A. Gottwald‡
*Department of Mathematics and Statistics, Surrey University, Guildford, GU2 7XH, United Kingdom*
(Received 1 March 2001; revised manuscript received 8 March 2002; published 14 June 2002)

A general model is introduced to describe a wave-envelope system for the situation when the linear dispersion relation has three branches, which in the absence of any coupling terms between these branches, would intersect pairwise in three nearly coincident points. The system contains two waves with a strong linear coupling between them, to which a third wave is then coupled. This model has two gaps in its linear spectrum. As is typical for wave-envelope systems, the model also contains a set of cubic nonlinear terms. Realizations of this model can be made in terms of temporal or spatial evolution of optical fields in, respectively, either a planar waveguide, or a bulk-layered medium resembling a photonic-crystal fiber, which carry a triple spatial Bragg grating. Another physical system described by the same general model is a set of three internal wave modes in a density-stratified fluid, whose phase speeds come into close coincidence for a certain wave number. A nonlinear analysis is performed for zero-velocity solitons, that is, they have zero velocity in the reference frame in which the third wave has zero group velocity. If one may disregard the self-phase modulation (SPM) term in the equation for the third wave, we find an analytical solution which shows that there simultaneously exist two different families of solitons: regular ones, which may be regarded as a smooth deformation of the usual gap solitons in a two-wave system, and *cuspons*, which have finite amplitude and energy, but a singularity in the first derivative at their center. Even in the limit when the linear coupling of the third wave to the first two nearly vanishes, the soliton family remains drastically different from that in the uncoupled system; in this limit, regular solitons whose amplitude exceeds a certain critical value are replaced by *peakons* (whose first derivative is finite at the center, but jumps in value). While the regular solitons, cuspons, and peakons are found in an exact analytical form, their stability is tested numerically, which shows that they all may be stable. If the SPM terms are retained, we find that there may again simultaneously exist two different families of generic stable soliton solutions, namely, regular ones and peakons. Direct simulations show that both types of solitons are stable in this case.

DOI: 10.1103/PhysRevE.65.066606 PACS number(s): 05.45.Yv, 42.65.Tg, 42.81.Dp, 47.55.Hd

## I. INTRODUCTION

### A. Model system

Gap solitons (GS) is a common name for solitary waves in nonlinear models which feature one or more [2] gaps in their linear spectrum, see review papers [1] and [2], respectively, for these two cases. A soliton may exist if its frequency belongs to the gap, as then it does not decay into linear waves.

Gaps in the linear spectrum are a generic phenomenon in two- or multi-component systems, as intersection of dispersion curves belonging to different components is generically prevented by a linear coupling between the components. Excluding cases when the system's linear spectrum is unstable (which is possible in a fluid dynamics application [3]), the intersection avoidance alters the spectrum so that a gap opens in place of the intersection. Approximating the two dispersion curves, that would intersect in the absence of the coupling, by straight lines, and assuming a generic cubic $[\chi^{(3)}]$ nonlinearity, one arrives at a generalized massive Thirring model (GMTM), which has a family of exact GS solutions that completely fill the gap [4]. The model has a direct application to nonlinear optics, describing copropagation of forward- and backward-traveling electromagnetic waves in a fiber with a resonant Bragg grating (BG). Gap solitons, first predicted theoretically, were observed in experiments with light pulses launched into a short piece of the BG-equipped fiber [5] (in fact, optical solitons that were first observed in the BG fiber [6] were, strictly speaking, not of the GS type, but more general ones, whose central frequency did not belong to the fiber's band gap).

GS are known not only in optics but also in other physical settings, for instance, in density-stratified fluid flows, where dispersion curves pertaining to two different internal-wave modes often exhibit near intersections. Again taking into regard weak nonlinearity, one can predict the occurrence of GS in density-stratified fluids [7].

In this work, we aim to consider GS that may exist in a generic situation of the next type, when the underlying system contains three wave components, and the corresponding dispersion curves intersect at three nearly coincident points,

*Email address: R.H.J.Grimshaw@lboro.ac.uk
†Email address: malomed@eng.tau.ac.il
‡Email address: g.gottwald@surrey.ac.uk

 

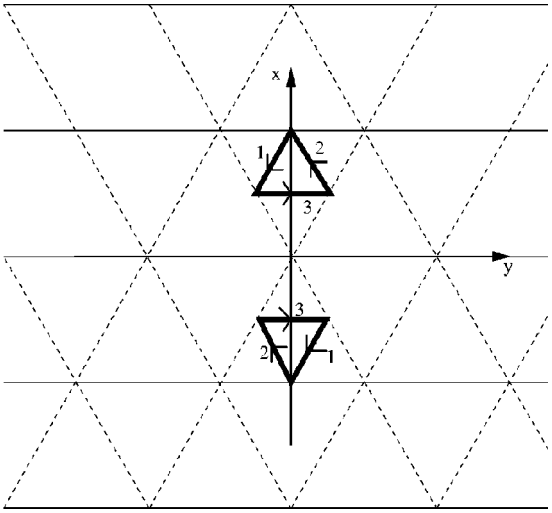


FIG. 1. A schematic representation of the optical model that gives rise to the three linearly coupled waves in a $\chi^{(3)}$ waveguide. The figure shows either the planar waveguide with the triple Bragg grating, in the case of the temporal evolution of the fields, or the transverse cross section of the bulk medium of the layered (photonic-crystal-fiber) type, in the case of the spatial evolution along the coordinate $z$ perpendicular to the plane of the figure. The triangles formed by bold arrows illustrate how the linear couplings between the three waves, whose Poynting vectors are represented by the arrows, are induced by the Bragg reflections on the three gratings. The difference between the gratings represented by the continuous and dashed lines is in their strength (refractive-index contrast).

unless linear coupling terms are taken into account. Situations of this type can readily occur in the above-mentioned density-stratified fluid flows, since tuning of two suitable external parameters can often lead to a near coincidence in the linear phase speeds of three independent internal wave modes, for certain wave numbers (see [8]). Indeed, similar considerations can be applied to many other physical systems. As for the usual GS systems, the generic wave-envelope model can be expected to contain cubic nonlinear terms.

In optics, a $\chi^{(3)}$-nonlinear model with three linearly coupled waves is possible too, in terms of either temporary evolution of fields in a planar nonlinear waveguide equipped with a *triple* BG in the form of three systems of parallel scores, or spatial evolution of stationary fields in a bulk waveguide with a similar triple BG consisting of three systems of parallel interfaces between layers. The latter realization seems natural enough, as it strongly resembles photonic-crystal fibers, which have recently attracted a great deal of interest [9]. Note that the former version of the model is a generalization of a three-wave model for a $\chi^{(2)}$-nonlinear planar waveguide with an ordinary BG, which was introduced in [10,11]. Both versions of the proposed model are illustrated in Fig. 1, where the periodic lattice shows the triple BG. In the case of the temporal evolution, Fig. 1 displays the planar waveguide, while in the case of the spatial evolution, it is a transverse cross section of the bulk waveguide.

We stress that the lattice in Fig. 1 is not completely symmetric; although the triangular cells of the lattice are equilateral ones, the two diagonal subgratings are assumed, in the general case, to have the strength (contrast of the refractive index) smaller than the horizontal one. The bold triangles inscribed into the two triangular cells illustrate the resonant Bragg reflections that give rise to linear couplings between the waves. Then, neglecting intrinsic dispersion or diffraction of the waves in comparison with the strong artificial dispersion/diffraction induced by the Bragg reflections, normalized equations governing the spatial evolution of the three fields whose Poynting vectors are shown by three bold arrows in Fig. 1, are

$$i\left(\frac{\partial u_1}{\partial t}-\frac{\partial u_1}{\partial x}-\frac{1}{\sqrt{3}}\frac{\partial u_1}{\partial y}\right)+u_2+\kappa u_3 +(|u_1|^2+2|u_2|^2+2|u_3|^2)u_1=0, \tag{1}$$

$$i\left(\frac{\partial u_2}{\partial t}+\frac{\partial u_2}{\partial x}-\frac{1}{\sqrt{3}}\frac{\partial u_2}{\partial y}\right)+u_1+\kappa^* u_3 +(|u_2|^2+2|u_1|^2+2|u_3|^2)u_2=0, \tag{2}$$

$$i\left(\frac{\partial u_3}{\partial t}+\frac{2}{\sqrt{3}}\frac{\partial u_3}{\partial y}\right)+\kappa^* u_1+\kappa u_2 +(|u_3|^2+2|u_1|^2+2|u_2|^2)u_3=\omega_0 u_3. \tag{3}$$

Here, the evolution variable $t$ is the proper time in the case of the temporal evolution in the planar waveguide, or the coordinate $z$ in the direction perpendicular to the plane of the figure in the case of the spatial evolution in the bulk waveguide. In the latter case, the beam enters the medium through the plane $z=0$ and evolves along the coordinate $z$, that is why it plays the role of the evolution variable in the equations (the initial conditions necessary to launch a soliton will be discussed in more detail below). The relative coefficients in front of the $x$- and $y$-derivative terms correspond to the geometry in Fig. 1, the coefficient of the walk off in the $x$ direction in the first two equations being normalized to be $\pm 1$. The coefficient of the BG-induced linear conversion between the waves $u_1$ and $u_2$ is normalized to be one, while the parameter $\kappa$ (which is complex, in the most general case, but see the discussion below) accounts for the linear conversion between these waves and the third wave $u_3$, and the usual ratio 1:2 between the coefficients of the self-phase modulation (SPM) and cross-phase modulation (XPM) is adopted. Last, $\omega_0$ is a frequency/wave-number mismatch between the third and the first two waves, which is caused by the above-mentioned asymmetry between the diagonal and horizontal subgratings, as well as by other reasons.

As we mentioned above, the Bragg constant $\kappa$ in Eqs. (1)–(3), which couples the field $u_3$ to the pair $u_{1,2}$, is complex in the general case [note that the constant of the Bragg coupling between the fields $u_1$ and $u_2$ might also be complex in its primary form, and making it equal to one in Eqs. (1) and (2) involves opposite constant phase shifts of the fields

$u_1$ and $u_2$, which is why $\kappa$ and $\kappa^*$ appear exactly as in Eqs. (1)–(3)]. However, assuming that each score, the families of which constitute the triple grating (in the case of the temporal-domain evolution in the planar waveguide), gives rise to simple reflection described by the classical Fresnel formulas, it is easy to conclude that all the coupling constants are real and positive, provided that either the light is polarized orthogonally to the waveguide's plane, and the reflection takes place from a less optically dense material (i.e., the ''score'' is, literally, a shallow trough on the surface of the planar waveguide), or the light is polarized parallel to the plane of the waveguide, and the reflection is from a more optically dense material. Similarly, in the case when the same equations describe the spatial evolution of the optical fields in the layered bulk medium, one may assume that either the light is polarized in the $z$ direction, and seams between the layers are filled with a material (for instance, air) which is optically less dense than the bulk medium, or the polarization is orthogonal to the $z$ axis (i.e., it is parallel to the plane of Fig. 1), and the material filling the interlayer seams is optically denser than the host medium.

In the present paper, we focus on this case, which was described above in detail for the realizations of the model in terms of both planar and bulk optical waveguides, and which corresponds to $\kappa$ real and positive in Eqs. (1)–(3). Note, incidentally, that the case when $\kappa$ is real and *negative* can be reduced to the same case simply by reversing the sign in the definition of $u_3$.

The model displayed in Fig. 1 may be further generalized by introducing an additional asymmetry, which will remove the equality between the horizontal side of the lattice's triangular cell and its diagonal sides. Then, the simultaneous fulfillment of the Bragg-reflection conditions for the waves $u_{1,2}$ and $u_3$ can be secured by making the waveguide anisotropic. However, such a generalization goes beyond the scope of this paper.

For the physical realization of the model, Eqs. (1)–(3) must be supplemented by initial conditions at $t=0$ in the case of the temporal evolution in the planar waveguide, or boundary conditions at $z=0$ in the case of the spatial evolution in the bulk medium. It is sufficient to assume that, at $t=0$, a single wave component (for instance, $u_3$) is launched into the waveguide. The linear-coupling terms in the equations will then start to generate the other components, and, if solitons that might exist in this model are stable (see below), they may self-trap from such an initial beam.

Bearing in mind also the above-mentioned application to internal waves in stratified fluids, as well as similar realizations in other physical media, Eqs. (1)–(3) may be naturally extended by introducing more general SPM and XPM coefficients, as in applications other than nonlinear optics, the ratios between the XPM and SPM coefficients may be different from those adopted above. Thus, the generalized system of equations takes the following form, in which we confine consideration to $y$-independent solutions (the consideration of possible three-dimensional solitons in the case of $y$-dependent fields is not an objective of this work):

$$i\left(\frac{\partial u_1}{\partial t}-\frac{\partial u_1}{\partial x}\right)+u_2+\kappa u_3 + \alpha(\alpha\sigma_1|u_1|^2+\alpha|u_2|^2+|u_3|^2)u_1=0, \tag{4}$$

$$i\left(\frac{\partial u_2}{\partial t}+\frac{\partial u_2}{\partial x}\right)+u_1+\kappa u_3 + \alpha(\alpha\sigma_1|u_2|^2+\alpha|u_1|^2+|u_3|^2)u_2=0, \tag{5}$$

$$i\frac{\partial u_3}{\partial t}+\kappa(u_1+u_2)+(\sigma_3|u_3|^2+\alpha|u_1|^2+\alpha|u_2|^2)u_3=\omega_0 u_3, \tag{6}$$

where, in accord with the discussion above, we set $\kappa$ to be real and positive.

The coefficients $\sigma_{1,3}$ and $\alpha$ in Eqs. (4)–(6) are the generalized SPM and XPM coefficients, respectively. In particular, $\alpha$ is defined as a relative XPM coefficient between the first two waves and the third wave. In fact, the coefficients $\sigma_1$ and $\sigma_3$ both may be normalized to be $\pm 1$, unless they are equal to zero; however, it will be convenient to keep them as free parameters, see below (note that the SPM coefficients are always positive in the optical models, but in those describing density-stratified fluids they may have either sign). In optical models, all the coefficients $\alpha$ and $\sigma_{1,3}$ are positive. However, in the models describing the internal waves in stratified fluids, there is no inherent restriction on their signs, and some of them may indeed be negative.

The symmetry between the walk-off terms in Eqs. (4) and (5) is not really essential, and we will comment later on the more general case when these terms are generalized as follows:

$$-\frac{\partial u_1}{\partial x}\to -c_1\frac{\partial u_1}{\partial x}, \quad +\frac{\partial u_2}{\partial x}\to +c_2\frac{\partial u_1}{\partial x}, \tag{7}$$

where $c_1$ and $c_2$ are different, but have the same sign. As for Eq. (6), it is obvious that the walk-off term in this equation, if any, can always be eliminated by means of a straightforward transformation.

We have kept only the most natural nonlinear SPM and XPM terms in Eqs. (4)–(6), i.e., the terms of the same types as in the standard GMT model. Additional terms, including nonlinear corrections to the linear couplings [e.g., a term $\sim|u_1|^2u_2$ in Eq. (4)] may appear in more general models, such as a model of a deep (strong) BG [10].

Equations (4)–(6) conserve the norm, which has the physical meaning of energy in optics,

$$N\equiv\sum_{n=1,2,3}\int_{-\infty}^{+\infty}|u_n(x)|^2dx, \tag{8}$$

the Hamiltonian,

$$H\equiv H_{\rm grad}+H_{\rm coupl}+H_{\rm focus}, \tag{9}$$

$$H_{\rm grad}\equiv\frac{i}{2}\int_{-\infty}^{+\infty}\left(u_1^*\frac{\partial u_1}{\partial x}-u_2^*\frac{\partial u_2}{\partial x}\right)dx+\text{c.c.}, \tag{10}$$

$$H_{\rm coupl} \equiv -\int_{-\infty}^{+\infty} [u_1^* u_2 + \kappa u_3^* (u_1 + u_2)] dx + \text{c.c.}, \quad (11)$$

$$H_{\rm focus} \equiv -\int_{-\infty}^{+\infty} \left[ \frac{1}{2} \alpha^2 \sigma_1 (|u_1|^4 + |u_2|^4) + \frac{1}{2} \sigma_3 |u_3|^4 + \alpha^2 |u_1|^2 |u_2|^2 + \alpha |u_3|^2 (|u_1|^2 + |u_2|^2) \right] dx, \quad (12)$$

and the momentum, which will not be used here. In these expressions, the asterisk and c.c. both stand for complex conjugation, $H_{\rm grad}$, $H_{\rm coupl}$, and $H_{\rm focus}$ being the gradient, linear-coupling, and self-focusing parts of the Hamiltonian. To obtain the Eqs. (4)–(6) from the Hamiltonian, the conjugate pairs of the variables are defined, in a standard fashion, as $u_n, u_n^*$.

Our objective is to find various types of solitons existing in the generic three-wave systems (4)–(6) and investigate their stability. Focusing first on the case (suggested by the analogy with GMTM) when the SPM term in Eq. (6) may be neglected (i.e., $\sigma_3 = 0$), in Sec. III we find a general family of zero-velocity solitons in an exact analytical form. We will demonstrate that they are of two drastically different types: regular GS, and *cuspons*, i.e., solitons with a cusp singularity at the center, in which the soliton amplitude is finite, but the derivative is infinite; further, the energy of the cuspons is finite. Cuspons are known to exist in degenerate models without linear terms (except for the evolution term such as $\partial u/\partial t$), i.e., without a linear spectrum, a well-known example being the exactly integrable Camassa-Holm (CH) equation [13,14] (see also [15]). Our model resembles the CH one in the sense that both give rise to coexisting solutions in the form of regular solitons and cuspons. The cause for the existence of these singular solitons in our model is the fact that, looking for a zero-velocity soliton solution, one may eliminate the field $u_3$ by means of an algebraic relation following, in this case, from Eq. (6). The subsequent substitution of that result into the first two Eqs. (4) and (5) produces a *rational* nonlinearity in them, the corresponding rational functions featuring a singularity at some (critical) value of the soliton's amplitude. If the amplitude of a regular-soliton solution is going to exceed the critical value, it actually cannot exist, and in the case when $\sigma_3 = 0$ it is replaced by a cuspon, whose amplitude is exactly equal to the critical value.

In the limit $\kappa \to 0$, which corresponds to the vanishing linear coupling between the first two and third waves, the cuspon resembles a *peakon*, which is a finite-amplitude solitary wave with a jump of its first derivative at the center. Note that peakon solutions, coexisting with regular solitons (this property is shared by our model), are known in a slightly different (also integrable) version of the CH equation, see, e.g., Refs. [13,16,17]. We also note that soliton solutions with a discontinuity in the first derivative have been found in the BG model (which does contain a linear part) in the case where the grating parameter changes abruptly [18].

Then, we show that, when the SPM term is restored in Eq. (6) [i.e., $\sigma_3 \neq 0$; the presence or absence of the SPM terms $\sim \sigma_1$ in Eqs. (4) and (5) is not crucially important], the system supports a different set of soliton solutions. These are regular GS and, depending on the sign of certain parameters, a family of peakons, which, this time, appear as generic solutions, unlike the case $\sigma_3 = 0$, when they only exist as a limiting form of the cuspon solutions corresponding to $\kappa \to 0$. As far as we know, the model formulated in the present paper is the first spatially uniform nondegenerate one (i.e., a model with a nonvanishing linear part) which yields both cuspons and peakons.

### B. Stability of solitons and spatiotemporal collapse

As concerns the dynamical stability of the various solitons in the models (4)–(6), in this work we limit ourselves to direct simulations, as a more rigorous approach, based on numerical analysis of the corresponding linear stability-eigenvalue problem [19], is technically difficult in the case of cuspons and peakons (results of such an analysis, based on the Evans-function technique, will be presented elsewhere). In fact, direct simulations of perturbed cuspons and peakons is a hard problem too, but we have concluded that identical results concerning the stability are produced (see Sec. III below) by high-accuracy finite-difference and pseudospectral methods (each being implemented in more than one particular form), which lends the results credibility. A general conclusion is that the regular solitons are always stable. As for the cuspons and peakons, they may be either stable or unstable.

If the cusp is strong enough, the numerical results presented below demonstrate that the instability of a cuspon initiates formation of a genuine singularity, i.e., onset of a *spatiotemporal collapse* [20] in the present one-dimensional model. Before proceeding to the consideration of solitons in the following sections, it is relevant to discuss collapse phenomenon in some detail.

A simple virial-type estimate for the possibility of the collapse can be done, assuming that the field focuses itself in a narrow spot with a size $(t)$, amplitude $\aleph(t)$, and a characteristic value $K(t)$ of the field's wave number [20]. The conservation of the norm (8) imposes a restriction $\aleph^2 L \sim N$, i.e., $L \sim N/\aleph^2$. Next, the self-focusing part (9) of the Hamiltonian (9), which drives the collapse, can be estimated as

$$H_{\rm focus} \sim -\aleph^4 L \sim -N\aleph^2. \quad (13)$$

On the other hand, the collapse can be checked by the gradient term (10) in the full Hamiltonian, that, in the same approximation, can be estimated as $H_{\rm grad} \sim \aleph^2 KL \sim NK$. Further, Eqs. (4)–(6) suggest an estimate $K \sim \aleph^2$ for a characteristic wave number of the wave field [the same estimate for $K$ follows from an expression (21) for the exact stationary-soliton solution given below], thus we have $H_{\rm grad} \sim N\aleph^2$. Comparing this with the expression (13), one concludes that the parts of the Hamiltonian promoting and inhibiting the

collapse scale the same way as $\aleph \to \infty$ (or $L \to 0$), hence a *weak collapse* [20] may be possible (but does not necessarily take place) in systems of the present type. We stress that, in one-dimensional models of GS studied thus far and based on GMTM, collapse has never been reported. The *real existence* of the collapse in the present one-dimensional three-wave GS model, which will be shown in detail below as a result of numerical simulations, is therefore a novel dynamical feature, and it seems quite natural that cuspons and peakons, in the case when they are unstable, play the role of catalysts stimulating the onset of the collapse. The possibility of a real collapse in a one-dimensional (1D) system is quite interesting by itself, and also because experimental observation of spatiotemporal self focusing in nonlinear optical media is a subject of considerable interest, see, e.g., Ref. [21].

## II. ANALYTICAL SOLUTIONS

### A. The dispersion relation

The first step in the investigation of the system is to understand its linear spectrum. Substituting $u_{1,2,3} \sim \exp(ikx - i\omega t)$ into Eqs. (4)–(6), and omitting nonlinear terms, we arrive at a dispersion equation,

$$(\omega^2 - k^2 - 1)(\omega - \omega_0) = 2\kappa^2(\omega - 1). \tag{14}$$

If $\kappa = 0$, the third wave decouples, and the coupling between the first two waves produces a commonly known gap, so that the solutions to Eq. (14) are $\omega_{1,2} = \pm\sqrt{1+k^2}$ and $\omega_3 = \omega_0$. If $\kappa \neq 0$, the spectrum can be easily understood by treating $\kappa$ as a small parameter. However, the following analysis is valid for all values of $\kappa$ in the range $0 < \kappa^2 < 1$.

First, consider the situation when $k = 0$. Three solutions of Eq. (14) are then

$$\omega = 1, \quad \omega = \omega_\pm \equiv (\omega_0 - 1)/2 \pm \sqrt{(\omega_0+1)^2/4 + 2\kappa^2}. \tag{15}$$

It can be easily shown that $\omega_- < \min\{\omega_0, -1\} \leqslant \max\{\omega_0, -1\} < \omega_+$, so that one always has $\omega_- < -1$, while $\omega_+ < 1$ if $\omega_0 < 1 - \kappa^2$, and $\omega_+ > 1$ if $\omega_0 > 1 - \kappa^2$. Next, it is readily seen that, as $k^2 \to \infty$, either $\omega^2 \approx k^2$, or $\omega \approx \omega_0$. Each branch of the dispersion relation generated by Eq. (14) is a monotonic function of $k^2$. Generic examples of the spectrum are shown in Fig. 2, where the panels (a) and (b) pertain, respectively, to the cases $\omega_0 < 1 - \kappa^2$ with $\omega_+ < 1$, and $\omega_0 > 1$ with $\omega_+ > 1$. The intermediate case, $1 - \kappa^2 < \omega_0 < 1$, is similar to that shown in panel (a), but with the points $\omega_+$ and 1 at $k = 0$ interchanged. When $\omega_0 < 1$, the upper gap in the spectrum is $\min\{\omega_+, 1\} < \omega < \max\{\omega_+, 1\}$, while the lower gap is $\omega_- < \omega < \omega_0$. When $\omega_0 > 1$, the upper gap is $\omega_0 < \omega < \omega_+$, and the lower one is $\omega_- < \omega < 1$.

### B. Gap solitons

The next step is to search for GS solutions to the full nonlinear system. In this work, we confine ourselves to the case of zero-velocity GS, substituting into Eqs. (4)–(6)

$$u_n(x,t) = U_n(x)\exp(-i\omega t), \quad n = 1,2,3, \tag{16}$$

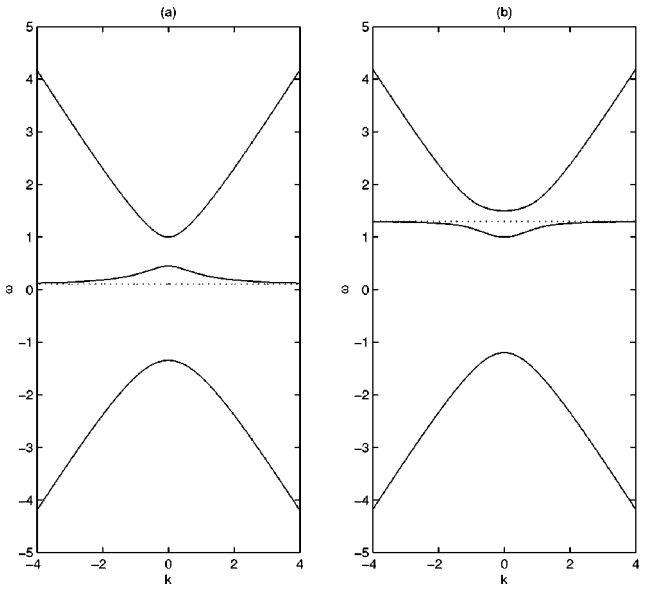


FIG. 2. Dispersion curves produced by Eq. (14) in the case $\kappa = 0.5$: (a) $\omega_0 < 1 - \kappa^2$; (b) $\omega_0 > 1$. The dashed line in each panel is $\omega = \omega_0$. The case with $1 - \kappa^2 < \omega_0 < 1$ is similar to case (a) but with the points $\omega_+$ and 1 at $k = 0$ interchanged.

where it is assumed that the soliton's frequency $\omega$ belongs to one of the gaps. In fact, even the description of zero-velocity solitons is quite complicated. Note, however, that if one sets $\kappa = 0$ in Eqs. (4)–(6), keeping nonlinear XPM couplings between the first two and third waves, the gap which exists in the two-wave GMT model remains unchanged, and the corresponding family of GS solutions does not essentially alter, in accord with the principle that nonlinear couplings cannot alter gaps or open a new one if the linear coupling is absent [12]; nevertheless, the situation is essentially different if $\kappa$ is vanishingly small, but not exactly equal to zero, see below.

The substitution of Eq. (16) into Eqs. (4) and (5) leads to a system of two ordinary differential equations for $U_1(x)$ and $U_2(x)$, and an algebraic relation for $U_3(x)$,

$$iU_1' = \omega U_1 + U_2 + \kappa U_3 + \alpha(\alpha\sigma_1|U_1|^2 + \alpha|U_2|^2 + |U_3|^2)U_1, \tag{17}$$

$$-iU_2' = \omega U_2 + U_1 + \kappa U_3 + \alpha(\alpha\sigma_1|U_2|^2 + \alpha|U_1|^2 + |U_3|^2)U_2, \tag{18}$$

$$(\omega_0 - \omega + \sigma_3|U_3|^2 + \alpha|U_1|^2 + \alpha|U_2|^2)U_3 = \kappa(U_1 + U_2), \tag{19}$$

where the prime stands for $d/dx$. To solve these equations, we substitute $U_{1,2} = A_{1,2}(x)\exp[i\phi_{1,2}(x)]$ with real $A_n$ and $\phi_n$. After substituting the expression (19) into Eqs. (17) and (18), and some simple manipulations, it can be found that $(A_1^2 - A_2^2)' = 0$ and $(\phi_1 + \phi_2)' = 0$. Using the condition that the soliton fields vanish at infinity, we immediately conclude that

$$A_1^2(x) = A_2^2(x) \equiv S(x); \tag{20}$$

as for the constant value of $\phi_1+\phi_2$, it may be set equal to zero without loss of generality, so that $\phi_1(x)=-\phi_2(x) \equiv \phi(x)/2$, where $\phi(x)$ is the relative phase of the two fields. After this, we obtain two equations for $S(x)$ and $\phi(x)$ from Eqs. (17) and (18),

$$\phi' = -2\omega - 2\cos\phi - 2\alpha^2(1+\sigma_1)S - S^{-1}U_3^2(\omega_0-\omega-\sigma_3 U_3^2), \tag{21}$$

$$S' = -2S\sin\phi - 2\kappa\sqrt{S}U_3\sin(\phi/2), \tag{22}$$

and Eq. (19) for the third wave $U_3$ takes the form of a cubic algebraic equation

$$U_3(\omega_0-\omega-2\alpha S-\sigma_3|U_3|^2) = 2\kappa\sqrt{S}\cos(\phi/2), \tag{23}$$

from which it follows that $U_3$ is a real-valued function.

This analytical consideration can be readily extended for more general Eqs. (4) and (5) that do not assume the symmetry between the waves $u_1$ and $u_2$, i.e., with the group-velocity terms in the equations altered as in Eq. (7). In particular, the relation (20) is then replaced by $c_1A_1^2(x) = c_2A_2^2(x) \equiv S(x)$. The subsequent analysis is similar to that above, and leads to results for the asymmetric model that are qualitatively similar to those presented below for the symmetric case.

Equations (21) and (22) have a Hamiltonian structure, as they can be represented in the form

$$\frac{dS}{dx} = \frac{\partial H}{\partial \phi}, \quad \frac{d\phi}{dx} = -\frac{\partial H}{\partial S}, \tag{24}$$

with the Hamiltonian

$$H = 2S\cos\phi + \alpha^2(1+\sigma_1)S^2 + 2\omega S + U_3^2(\omega_0-\omega-2\alpha S) - \frac{3}{2}\sigma_3 U_3^4, \tag{25}$$

which is precisely a reduction of the Hamiltonian (9) of the original systems (4)–(6) for the solutions of the present type. Note that $H$ is here regarded as a function of $S$ and $\phi$, and the relation (23) is regarded as determining $U_3$ in terms of $S$ and $\phi$. We stress that the dependence $U_3(S,\phi)$ was taken into account when deriving the Hamiltonian representation (24).

For soliton solutions, the boundary conditions at $x=\pm\infty$ yield $H=0$ so that the solutions can be obtained in an implicit form,

$$2S\cos\phi + \alpha^2(1+\sigma_1)S^2 + 2\omega S + U_3^2(\omega_0-\omega-2\alpha S) - (3/2)\sigma_3 U_3^4 = 0. \tag{26}$$

In principle, one can use the relations (23) and (26) to eliminate $U_3$ and $\phi$ and so obtain a single equation for $S$. However, this is not easily done unless $\sigma_3=0$ [no SPM term in Eq. (6)], and so we proceed to examine this special, but important, case first. Note that the no-SPM case also plays an important role for GMTM, which is exactly integrable by means of the inverse scattering transform just in this case [1].

### C. Cuspons, the case $\sigma_3=0$

Setting $\sigma_3=0$ makes it possible to solve Eq. (23) for $U_3$ explicitly in terms of $S$ and $\phi$,

$$U_3 = \frac{2\kappa\sqrt{S}\cos(\phi/2)}{\omega_0-\omega-2\alpha S}. \tag{27}$$

For simplicity, we also set $\sigma_1=0$ in Eqs. (4) and (5) and subsequent equations, although the latter assumption is not crucially important for the analysis developed below. Indeed, the analysis is based on the fact that the field $U_3$ can be explicitly eliminated by means of Eq. (27), which is not affected by $\sigma_1$. If $\sigma_1$ is kept in the system, it merely renormalizes some coefficients in the formulas derived below.

At the next step, one can also eliminate $\phi$, using Eqs. (26) and (27), to derive a single equation for $S$,

$$(dS/dx)^2 = 4S^2F(S), \tag{28}$$

$$F(S) \equiv \left(1-\omega-\frac{1}{2}\alpha^2 S\right) \times \left[2\left(1+\frac{\kappa^2}{\omega_0-\omega-2\alpha S}\right) - \left(1-\omega-\frac{1}{2}\alpha^2 S\right)\right]. \tag{29}$$

The function $F(S)$ has either one or three real zeros $S_0$. One is

$$S_{01} = 2(1-\omega)/\alpha^2, \tag{30}$$

and the remaining two, if they exist, are real roots of the quadratic equation,

$$(2+2\omega+\alpha^2 S_0)(\omega_0-\omega-2\alpha S_0) + 4\kappa^2 = 0. \tag{31}$$

Only the smallest positive real root of Eq. (31), to be denoted $S_{02}$ (if such exists), will be relevant below. Note, incidentally, that $F(S)$ cannot have double roots. It is easy to see that a consequence of this fact is that Eq. (28) cannot generate kink solutions, which have different limits as $x\to\pm\infty$, for both of which the right-hand side of Eq. (28) must have a double zero.

For a bright-soliton solution of Eq. (28), we need first that $F(0)>0$ (in this paper, we do not consider dark solitons, nor ''antidark'' solitons, i.e., solitons on top of a finite-amplitude flat background, a reason being that there is little chance that the flat background would be modulationally stable). Comparing the condition $F(0)>0$ with the expressions given in Sec. II A for the gaps in the linear spectrum, it is readily shown that this condition is exactly equivalent to requiring that $\omega$ belongs to either the upper or the lower gap of the linear spectrum. We note that the coupling to the third wave gives rise to nonlinearity of the rational type in the expression (29), despite the fact that the underlying systems (4)–(6) contain only cubic polynomial nonlinear terms. Even if the coupling constant $\kappa$ is small, it is clear that the rational nonlinearity may produce a strong effect in a vicinity of a *critical value* of the squared amplitude at which the denominator in the expression (29) vanishes,

$$S_{cr}=(\omega_0-\omega)/2\alpha, \tag{32}$$

where one must have $\alpha(\omega_0-\omega)>0$ (otherwise, this critical value is not relevant).

If $S_{cr}>0$, the structure of the soliton crucially depends on whether, with an increase of $S$, the function $F(S)$ defined by Eq. (29) first reaches zero at $S=S_0>0$ (i.e., either $S=S_{01}$ or $S=S_{02}$, whichever is the smaller positive value), or, instead, it first reaches the singularity at $S=S_{cr}$, i.e., whether $0<S_0<S_{cr}$, or $0<S_{cr}<S_0$. In the former case, the existence of $S_{cr}$ plays no role, and the soliton is a regular one, having the amplitude $\sqrt{S_0}$. This soliton may be regarded as obtained by a smooth deformation from the usual GS known in GMTM at $\kappa=0$.

In the case $0<S_{cr}<S_0$, as the soliton cannot have an amplitude larger than $\sqrt{S_{cr}}$, the amplitude takes this critical value. The soliton is singular in this case, being a *cuspon* (see details below), but, nevertheless, it is an absolutely relevant solution. The remaining possibilities are that either $S_{cr}<0$ and $S_0>0$, or vice versa; then the soliton may only be, respectively, regular or singular. Of course no soliton exists if both $S_0$ and $S_{cr}$ are negative. Further, using the symmetries of the equations, it is readily shown that for all these soliton solutions, $S(x)$ is symmetric about its center, which may be set at $x=0$, that is, $S(x)$ is an even function of $x$. For the cuspon solutions, and for those regular solutions whose squared amplitude is $S_{01}$, it can also be shown that the phase variable $\psi(x)=\phi(x)-\pi$ and $U_3(x)$ are odd functions of $x$, while for those regular solutions whose squared amplitude is $S_{02}$ the phase variable $\phi(x)$ and $U_3(x)$ are, respectively, odd and even functions of $x$.

It is now necessary to determine which parameter combinations in the set $(\omega,\omega_0,\alpha)$ permit the options described above. The most interesting case occurs when $\omega_0>\omega$ (so that $\omega$ belongs to the lower gap, see Fig. 2) and $\alpha>0$ (the latter condition always holds in the applications to nonlinear optics). In this case, it can be shown that the root $S_{02}$ of Eq. (31) is not relevant, and the options are determined by the competition between $S_{01}$ and $S_{cr}$. The soliton is a cuspon $(0<S_{cr}<S_{01})$ if

$$\alpha(\omega_0-\omega)<4(1-\omega). \tag{33}$$

In effect, the condition (33) sets an upper bound on $\alpha$ for given $\omega_0$ and $\omega$. In particular, this condition is always satisfied if $0<\alpha<4$.

If, on the other hand, the condition (33) does not hold (i.e., $0<S_{01}<S_{cr}$), we obtain a regular soliton. In a less physically relevant case, when again $\omega_0>\omega$ but $\alpha<0$, cuspons do not occur [as this time $S_{cr}<0$, see Eq. (32)], and only regular solitons may exist.

Next we proceed to the case $\omega_0<\omega$, so that $\omega$ is located in the upper gap of the linear spectrum. For $\alpha>0$, we have $S_{cr}<0$, hence, only regular solitons may occur, and indeed in this case there is always at least one positive root $S_0$, so a regular soliton does exist. If $\alpha<0$, then we have $S_{cr}>0$, but if $\omega_0<1-\kappa^2$ (when also $\omega<1$), there is at least one positive root $S_0<S_{cr}$; thus, only a regular soliton can exist in this case too. On the other hand, if $\alpha<0$ and $\omega_0>1-\kappa^2$ (and then $\omega>1$), there are no positive roots $S_0$, and so only cuspons occur.

Let us now turn to a detailed description of the cuspon's local structure near its center, when $S$ is close to $S_{cr}$. From the above analysis, one sees that cuspons occur whenever $\omega$ lies in the lower gap, with $\omega_0>\omega$ and $\alpha>0$, so that the criterion (33) is satisfied, or when $\omega$ lies in the upper gap with $1-\kappa^2<\omega_0<\omega$ and $\alpha<0$. To analyze the structure of the cuspon, we first note that, as it follows from Eq. (26), one has $\cos\phi=-1$ (i.e., $\phi=\pi$) when $S=S_{cr}$, which suggest to set

$$S_{cr}-S\equiv\delta(\kappa^2 R), \quad 1+\cos\phi\equiv\delta\rho, \tag{34}$$

where $\delta$ is a small positive parameter, and the stretched variables $R$ and $\rho$ are positive. At the leading order in $\delta$, it then follows from Eq. (26) that $\rho=\rho_0 R$, where

$$\rho_0\equiv\alpha^3(S_{01}-S_{cr}). \tag{35}$$

As it follows from the above analysis, $\rho_0$ is always positive for a cuspon. We also stretch the spatial coordinate, defining $x\equiv\delta^{3/2}\kappa^2 y$, the soliton center being at $x=0$. Since $S(x)$ is an even function of $x$, it is sufficient to set $x>0$ in this analysis. Then, on substituting the first relation from Eq. (34) into Eq. (28), we get, to the leading order in $\delta$, an equation

$$R(dR/dy)^2=\rho_0 S_{cr}^2/\alpha^2\equiv K^2, \tag{36}$$

so that

$$R=(3Ky/2)^{2/3}. \tag{37}$$

Note that in the original unstretched variables, the relation (37) shows that, near the cusp,

$$S_{cr}-S(x)\approx(3K\kappa x/2)^{2/3}, \tag{38}$$

$$dS/dx\approx(2/3)^{1/3}(K\kappa)^{2/3}x^{-1/3}, \tag{39}$$

and it follows from Eq. (27) that $U_3$ is unbounded near the cusp,

$$U_3\approx(S_{cr}/\alpha)(2\alpha\rho_0 K^2/3\kappa x)^{1/3}. \tag{40}$$

In particular, Eq. (39) implies that, as $K\kappa$ decreases, the cusp gets localized in a narrow region where $|x|\lesssim K^2\kappa^2$ (outside this region, $|dS/dx|$ is bounded and shows no cusp). Note that this limit can be obtained either as $\kappa^2\to 0$, or as $\rho_0\to 0$ [recall that $\rho_0$ is defined in Eq. (35)].

An example of the cuspon is shown in Fig. 3. Although the first derivative in the cuspon is singular at its center, as it follows from Eq. (39) [see also Fig. 3(a)], and its $U_3$ component diverges at $x\to 0$ as per Eq. (40), it is easily verified that the value of the Hamiltonian (9) [and, obviously, the value of the norm (8) too] is finite for the cuspon solution. These solitons are similar to cuspons found as exact solutions to the Camassa-Holm (CH) equation [13,14], which have a singularity of the type $|x|^{1/3}$ or $|x|^{2/3}$ as $|x|\to 0$, cf. Eqs. (38) and (39). The CH equation is integrable, and it is

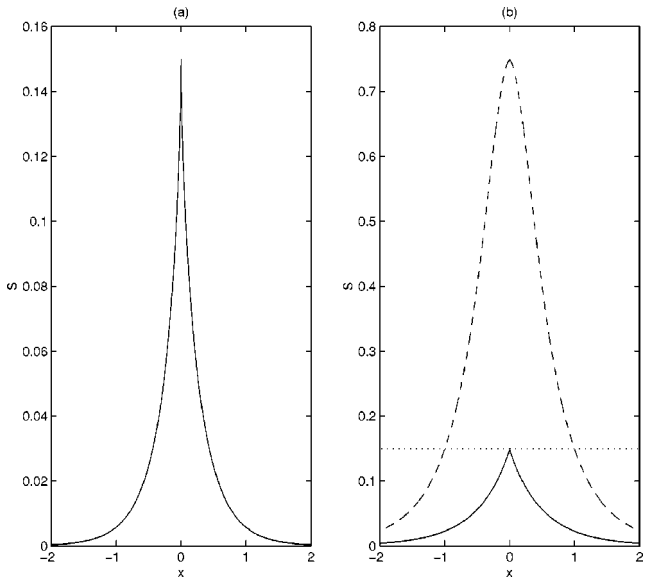


FIG. 3. The shape of the cuspon for $\alpha=2.0$, $\omega_0=0.1$, $\omega=-0.5$, and (a) $\kappa=0.5$, i.e., in the general case, and (b) $\kappa=0.1$, i.e., for small $\kappa$. In case (b) we also show the usual gap soliton (by the dashed line), the part of which above the critical value $S=S_{\rm cr}$ (shown by the dotted line) should be removed and the remaining parts brought together to form the peakon corresponding to $\rho_0\kappa^2\to 0$.

degenerate in the sense that it has no linear terms except for $\partial u/\partial t$ (which makes the existence of the solution with a cusp singularity possible). Our three-wave system (4)–(6) is not degenerate in that sense; nevertheless, the cuspon solitons are possible in it because of the model's multicomponent structure: the elimination of the third component generates the nonpolynomial nonlinearity in Eqs. (17) and (18), and, finally, in Eqs. (22) and (28), which gives rise to the cusp. It is noteworthy that, as well as the CH model, ours gives rise to two different *coexisting* families of solitons, viz., regular ones and cuspons. It will be shown below that the solitons of both types may be stable.

Of course, the presence of the singularities in $U_3(x)$ and $dS/dx$ at $x\to 0$ suggests that higher-order terms, such as the higher-order dispersion, should be taken into regard in this case. The fact that the cuspon's Hamiltonian converges despite these singularities, as well as a direct analysis, suggest that such higher-order terms will smooth the shape of the cuspon in a very narrow layer for small $x$, allowing for large but not diverging values of the fields. However, the small higher-order terms will not essentially alter the global shape of the cuspons. In the next section we will show that, in fact, the genuine generic singular solitons are (in the presence of the SPM terms) peakons, for which the singularities are much weaker, hence, the latter issue is still less significant. Besides that, it appears to be an issue of principal interest to understand what types of solitons the system may generate without intrinsic dispersion (cf. the situation for the traditional GMTM, in which the spectrum of soliton solutions is completely altered by the addition of intrinsic dispersion [22]).

In the special case $\kappa\ll 1$, when the third component is weakly coupled to the first two in the linear approximation (in terms of the optical model represented by Fig. 1, it is the case when the subgratings shown by the dashed lines are very weak), straightforward inspection of the above results shows that the cuspons look like *peakons*; that is, except for the above-mentioned narrow region of the width $|x|\sim\kappa^2$, where the cusp is located, they have the shape of a soliton with a discontinuity in the first derivative of $S(x)$ and a jump in the phase $\phi(x)$, which are the defining features of peakons ([13,16]). A principal difference of true peakons from cuspons is that the first derivative does not diverge inside a peakon, but is of course, discontinuous.

An important result of our analysis is that the family of solitons obtained in the limit $\kappa\to 0$ is drastically different from that in the model where one sets $\kappa=0$ from the very beginning. In particular, in the most relevant case, with $\omega_0>\omega$ and $\alpha>0$, the family corresponding to $\kappa\to 0$ contains regular solitons whose amplitude is smaller than $\sqrt{S_{\rm cr}}$; however, the solitons whose amplitude at $\kappa=0$ is larger than $\sqrt{S_{\rm cr}}$, i.e., the ones whose frequencies belong to the range (33) [note that the definition of $S_{\rm cr}$ does not depend on $\kappa$ at all, see Eq. (32)], are replaced by the peakons which are constructed in a very simple way: drop the part of the usual soliton above the critical level $S=S_{\rm cr}$, and bring together the two symmetric parts which remain below the critical level, see Fig. 3(b).

It is interesting that peakons are known as exact solutions to a version of the integrable CH equation slightly different from that which gives rise to the cuspons. As well as in the present system, in that equation the peakons coexist with regular solitons [16]. In the next section, we demonstrate that the peakons, which are found only as limit-form solutions in the no-SPM case $\sigma_3=0$, become generic solutions in the case $\sigma_3\neq 0$.

### D. Peakons, the case $\sigma_3\neq 0$

A natural question is whether the cuspon solutions are *structurally stable*, i.e., if they will persist on inclusion of terms that were absent in the analysis presented above (the other type of the stability, viz., dynamical stability against small initial perturbations, will be considered in the next section). Here, we address this issue by restoring the SPM term in Eq. (6), that is, we now set $\sigma_3\neq 0$, but assume that it is a small parameter. Note that, in the application to nonlinear optics, one should expect that $\sigma_3>0$, but there is no such restriction on the sign of $\sigma_3$ in the application to the flow of a density-stratified fluid. We still keep $\sigma_1=0$, as the inclusion of the corresponding SPM terms in Eqs. (4) and (5) amounts to trivial changes both in the above analysis, and in that presented below. On the other hand, we show below that the inclusion of the SPM term in Eq. (6) is a structural perturbation which drastically changes the character of the soliton solutions.

In view of the above results concerning the cuspons, we restrict our discussion here to the most interesting case when $S(x)$ is an even function of $x$, while $\psi(x)=\phi(x)-\pi$ and $U_3(x)$ are odd functions. In principle, one can use the relations (23) and (26) to eliminate $\phi$ and $U_3$ and so obtain a

single equation for $S$ [a counterpart to Eq. (28)], as it was done above when $\sigma_3=0$. However, when $\sigma_3\neq 0$, it is not possible to do this explicitly. Instead, we shall develop an asymptotic analysis valid for $x\to 0$, which will be combined with results obtained by direct numerical integration of Eqs. (21) and (22), subject of course to the constraints (23) and (26). Since singularities only arise at the center of the soliton (i.e., at $x=0$) when $\sigma_3=0$, it is clear that the introduction of a small $\sigma_3\neq 0$ will produce only a small deformation of the soliton solution in the region where $x$ is bounded away from zero.

First, we consider regular solitons. Because the left-hand side of Eq. (23) is not singular at any $x$, including the point $x=0$, when $\sigma_3=0$, we expect that regular solitons survive a perturbation induced by $\sigma_3\neq 0$. Indeed, if there exists a regular soliton, with $S_0\equiv S(x=0)$, and $\phi(x=0)=\pi$ and $U_3(x=0)=0$, it follows from Eq. (26) that the soliton's amplitude remains exactly the same as it was for $\sigma_3=0$, due to the fact that the regular soliton has $U_3(x=0)=0$.

Next, we turn to the possibility of singular solutions, that is, cuspons or peakons. Since we are assuming that $S_0=S(x=0)$ is finite, and that $\phi(x=0)=\pi$, it immediately follows from Eq. (23) that when $\sigma_3\neq 0$, $U_3$ must remain finite for all $x$, taking some value $U_0\neq 0$, say, as $x\to +0$. Since $U_3$ is an odd function of $x$, and $U_0\neq 0$, there must be a discontinuity in $U_3$ at $x=0$, i.e., a jump from $U_0$ to $-U_0$. This feature is in marked contrast to the cuspons for which $U_3$ is infinite at the center, see Eq. (40). Further, it then follows from Eq. (22) that, as $x\to 0$, there is also a discontinuity in $dS/dx$, with a jump from $2\kappa U_0\sqrt{S_0}$ to $-2\kappa U_0\sqrt{S_0}$. Hence, if we can find soliton solutions of this type, with $U_0\neq 0$, they are necessarily *peakons*, and we infer that cuspons do *not* survive the structural perturbation induced by $\sigma_3\neq 0$.

Further, if we assume that $U_0\neq 0$, then Eq. (23), taken in the limit $x\to 0$, immediately shows that

$$2\alpha(S_{\rm cr}-S_0)=\sigma_3 U_0^2 \tag{41}$$

[recall that $S_{\rm cr}$ is defined by Eq. (32)]. Next, the Hamiltonian relation (26), also taken in the limit $x\to 0$, shows that

$$-\frac{\rho_0}{\alpha}S_0-\alpha^2 S_0(S_{\rm cr}-S_0)=\frac{1}{2}\sigma_3 U_0^4, \tag{42}$$

where we have used Eq. (41) [recall that $\rho_0$ is defined by Eq. (35)]. Elimination of $U_0$ from Eqs. (41) and (42) yields a quadratic equation for $S_0$, whose positive roots represent the possible values of the peakon's amplitude.

We recall that for a cuspon which exists at $\sigma_3=0$ one has $\rho_0>0$, i.e., the amplitude of the corresponding formal regular soliton exceeds the critical value of the amplitude, see Eq. (35). Then, if we retain the condition $\rho_0>0$, it immediately follows from Eqs. (41) and (42) that no peakons may exist if the SPM coefficient in Eq. (6) is positive, $\sigma_3>0$. Indeed, Eq. (41) shows that $S_{\rm cr}-S_0>0$ if $\sigma_3>0$, which, along with $\rho_0>0$, leads to a contradiction in the relation (42).

Further, it is easy to see that a general condition for the existence of peakons following from Eqs. (41) and (42) is

$$\sigma_3\rho_0<0, \tag{43}$$

hence, peakons are possible if $\sigma_3<0$, or if we keep $\sigma_3>0$ but allow $\rho_0<0$. In the remainder of this section, we will show that peakons may exist only if $\rho_0>0$. Hence, it follows from the necessary condition (43) that peakons may indeed be possible solely in the case $\sigma_3<0$. On the other hand, regular solitons do exist in the case $\sigma_3>0$ (i.e., in particular, in nonlinear-optics models), as they have $U_0=0$, hence, neither Eq. (41) nor its consequence in the form of the inequality (43) apply to regular solitons. The existence of (stable) peakons for $\sigma_3<0$, and of (also stable) regular solitons for $\sigma_3>0$ will be confirmed by direct numerical results presented in the next section.

To obtain a necessary condition (which will take the form of $\rho_0>0$) for the existence of the peakons, we notice that the existence of any solitary wave implies the presence of closed dynamical trajectories in the phase plane of the corresponding dynamical system, which is based on the ordinary differential Eqs. (21) and (22), supplemented by the constraint (23). Further, at least one stable fixed point (FP) must exist inside such closed trajectories, therefore the existence of such a stable FP is a necessary condition for the existence of any solitary wave.

The FPs are found by equating to zero the right-hand sides of Eqs. (21) and (22), which together with Eq. (23) give three equations for the three coordinates $\phi, S$ and $U_3$ of the FP. First of all, one can find a trivial unstable FP of the dynamical system,

$$\cos\phi=-\frac{\omega+\kappa^2/(\omega_0-\omega)}{1+\kappa^2/(\omega_0-\omega)}, \quad S=0,$$

which does not depend on $\sigma_3$. Then, three nontrivial FPs can be found, with their coordinates $\phi_*$, $S_*$, and $U_{3*}$ given by the following expressions:

$$\phi_*^{(1)}=\pi, \quad S_*^{(1)}=\frac{1-\omega}{\alpha^2}=\frac{1}{2}S_{01}, \quad U_{3*}^{(1)}=0, \tag{44}$$

$$\phi_*^{(2)}=\pi, \quad (2-\sigma_3)S_*^{(2)}=2S_{\rm cr}-\frac{\sigma_3}{2}S_{01},$$

$$(2-\sigma_3)[\alpha U_{3*}^{(2)}]^2=\rho_0-\alpha^3 S_{\rm cr}, \tag{45}$$

$$(2-\sigma_3)S_*^{(3)}=2S_{\rm cr}-\frac{1}{2}\sigma_3 S_{01}+\frac{\kappa^2}{\alpha},$$

$$(2-\sigma_3)[\alpha U_{3*}^{(3)}]^2=\rho_0-\alpha^3 S_{\rm cr}-\alpha^2\kappa^2,$$

$$\cos(\phi_*^{(3)}/2)=-\frac{1}{2}\kappa U_{3*}^{(3)}/\sqrt{S_*^{(3)}}, \tag{46}$$

where the superscript is a number label for the FP. To be specific, we now consider the case of most interest, when both $S_{01}>0$ and $S_{\rm cr}>0$. In this case, the FP given by Eqs. (44) exists for all $\sigma_3$ and all $\rho_0$. However, for small $\sigma_3$ (in fact $\sigma_3<2$ is enough) and small $\kappa$, the FPs given by Eqs.

(45) and (46) exist only when $\rho_0>0$. Indeed, they exist only for $\rho_0>\alpha^3 S_{01}$ and $\rho_0>\alpha^3 S_{01}+\kappa^2$, respectively, or, on using the definition (35) of $\rho_0$, when $S_{01}>2S_{\rm cr}$ and $S_{01}>2S_{\rm cr}+\kappa^2/\alpha$, respectively.

Let us first suppose that $\rho_0<0$. Then there is only the single nontrivial FP, namely, the one given by Eqs. (44). This FP is clearly associated with the regular solitons, whose amplitude at the crest is $S_{01}$. Hence, we infer that for $\rho_0<0$ there are no other solitary-wave solutions, and in particular, no peakons (and no cuspons when $\sigma_3=0$ either, in accordance with what we have already found in Sec. II C above). When combined with the necessary condition (43) for the existence of peakons, we infer that there are no peakons when $\sigma_3>0$, thus excluding peakons from applications to the nonlinear-optics models, where this SPM coefficient is positive. However, peakons may occur in density-stratified fluid flows, where there is no inherent restriction on the sign of $\sigma_3$. This case is considered below, but first we note that in the case $\rho_0<0$ and $\sigma_3>0$ (which includes the applications to nonlinear optics), the same arguments suggest that there may be *periodic* solutions with a peakon-type discontinuity at the crests; indeed, our numerical solutions of the systems (21) and (22) show that this is the case.

Next, we suppose that $\rho_0>0$. First, if $S_{01}<2S_{\rm cr}$ then there is again the single nontrivial FP given by Eq. (44). But now, by analogy with the existence of cuspons when $\rho_0>0$ and $\sigma_3=0$, we infer that the solitary wave solution which is associated with this fixed point is a peakon, whose squared amplitude $S_0$ for small $\sigma_3$ is close to $S_{\rm cr}$, while the FP has $S_*^{(1)}=S_{01}/2<S_{\rm cr}$.

If, on the other hand, $S_{01}>2S_{\rm cr}$, the FPs given by Eqs. (45) and (46) become available as well. We now infer that the peakon solitary-wave solution continues to exist, and for sufficiently small $\sigma_3$ and $\kappa$ it is associated with the FP given by Eq. (45). Although Eq. (45) implies that $S_*^{(2)}\approx S_{\rm cr}$, and the peakon's squared amplitude $S_0$, determined by Eqs. (41) and (42), is also approximately equal to $S_{\rm cr}$, we nevertheless have $S_0>S_*^{(2)}$ as required. Note that, in the present case, the FPs given by Eqs. (44) and (46) lie outside the peakon's homoclinic orbit. In Fig. 4, we show a plot of a typical peakon obtained, in this case, by numerical solution Eqs. (21) and (22).

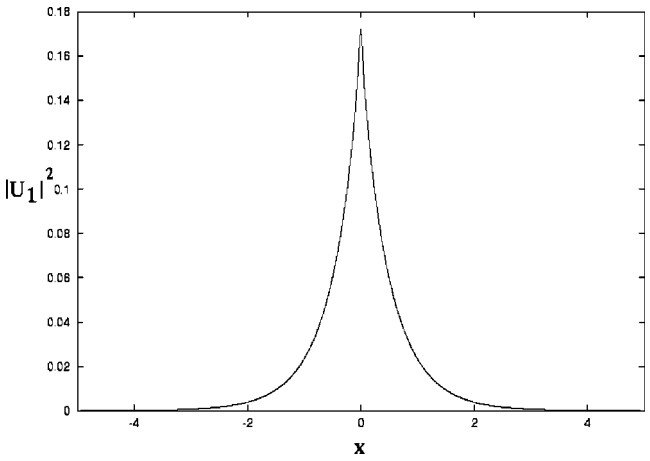


FIG. 4. The shape of the peakon for the case when $\sigma_3<0$, where we plot $|U_1|^2$. The parameters are $\sigma_3=-0.01$, $\kappa=0.1$, $\alpha=2.0$, $\omega_0=0.1$, and $\omega=-0.5$. In this case, $\rho_0=4.8$.

## III. NUMERICAL RESULTS

### A. Simulation techniques

The objectives of direct numerical simulations of the underlying Eqs. (4)–(6) were to check the dynamical stability of regular solitons, cuspons, and peakons in the case $\sigma_3=0$, and the existence and stability of peakons in the more general case, $\sigma_3\neq 0$. Both finite-difference and pseudospectral numerical methods have been used, in order to check that the same results are obtained by methods of both types. We used semi-implicit Crank-Nicholson schemes, in which the nonlinear terms were treated by means of the Adams-Bashforth method.

The presence of singularities required a careful treatment of cuspon and peakon solutions. To avoid numerical instabilities due to discontinuities, we found it, sometimes, beneficial to add an artificial weak high-wave-number viscosity to the pseudospectral code. This was done by adding linear damping terms to the right-hand side of Eqs. (4), (5), and (6), which have the form $-i\nu(k)k^2\hat{u}_n$ in the Fourier representation, where $\hat{u}_n$ is the Fourier transform of $u_n$ $(n=1,2,3)$. The high-pass filter viscosity $\nu(k)$ suppresses only high wave numbers and does not act on others. In particular, we chose

$$\nu(k)=\begin{cases} 0 & \text{if } |k|<\dfrac{5}{16}K, \\ \eta\left(\dfrac{16|k|}{K}-5\right) & \text{if } \dfrac{5}{16}K<|k|<\dfrac{3}{8}K, \\ \eta & \text{if } |k|>\dfrac{3}{8}K, \end{cases}$$

where $K$ is the largest wave number in the actual numerical scheme, and $\eta$ is a small viscosity coefficient. We have found that $\eta\sim 10^{-5}$ was sufficient to avoid Gibbs' phenomenon in long-time simulations.

When instabilities occur at a singular point (cusp or peak), it is hard to determine whether the instability is a real one, or a numerical artifact. Therefore, we checked the results by means of a finite-difference code which used an adaptive staggered grid; motivated by the analysis of the vicinity of the point $x=0$ reported above, we introduced the variable $\xi\equiv x^{2/3}$ to define an adaptive grid, and also redefined $U_3\equiv\sqrt{\xi}\tilde{U}_3$. In these variables, the cusp becomes a regular point. This approach was solely used to check the possible occurrence of numerical instabilities.

In the following sections we present typical examples of the numerical results for both cases considered above, viz., $\sigma_3=0$ and $\sigma_3<0$, when, respectively, cuspons and peakons are expected.

### B. Case $\sigma_3=0$

First, we report results obtained for the stability of regular solitary waves in the case $\sigma_3=0$. As initial configurations,

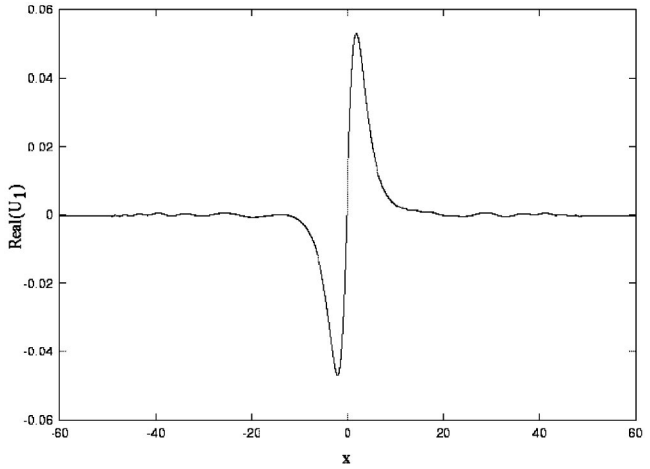


FIG. 5. The shape of an initially perturbed regular soliton in the case $\sigma_3=0$ at $t=5$, which illustrates the stabilization of the soliton through the shedding of small-amplitude radiated waves. The plot displayed is the field $\mathrm{Re}\,U_1(x)$. The parameters are $\kappa=0.01$, $\alpha=1.0$, $\omega_0=0.2$, and $\omega=0.9$.

we used the corresponding stationary solutions to Eqs. (21) and (22). To test the stability of the regular solitary waves, we added small perturbations to them. As could be anticipated, the regular solitary wave sheds off a small dispersive wave train and relaxes to a stationary soliton, see Fig. 5 (for a more detailed illustration of the generation of small radiated waves by a soliton, see also Fig. 8 below). If, however, a regular soliton is taken as an initial condition for parameter values inside, but close to the border of the cuspon region, it does not become unstable in this slightly modified section of parameter space (which only supports cuspons), but instead this soliton exhibits persistent internal vibrations, see an example in Fig. 6. These and many other simulations clearly show that the regular soliton is always stable, and, close to the parameter border with cuspons, it has a persistent internal mode.

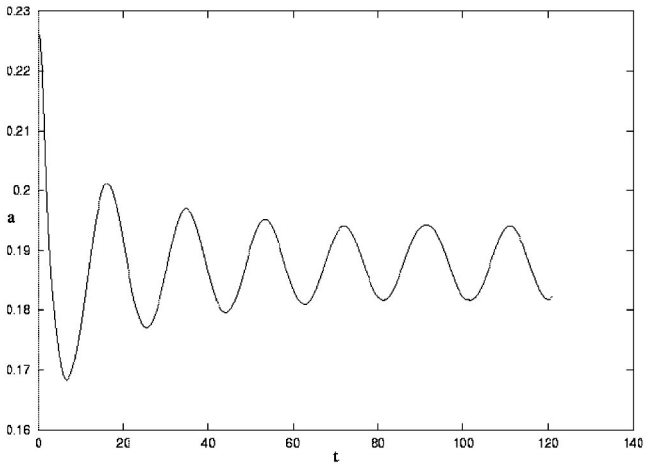


FIG. 6. Internal vibrations of an initially perturbed regular soliton, which was taken close to the parameter boundary of the cuspon region. The plot shows the squared amplitude $a\equiv|U_1(x=0)|^2$ of the $U_1(x)$ field versus time. The parameters are $\kappa=0.01$, $\alpha=1.9$, $\omega_0=1.5$, and $\omega=0.5$, with $\rho_0=0.095$ [see Eq. (35)].

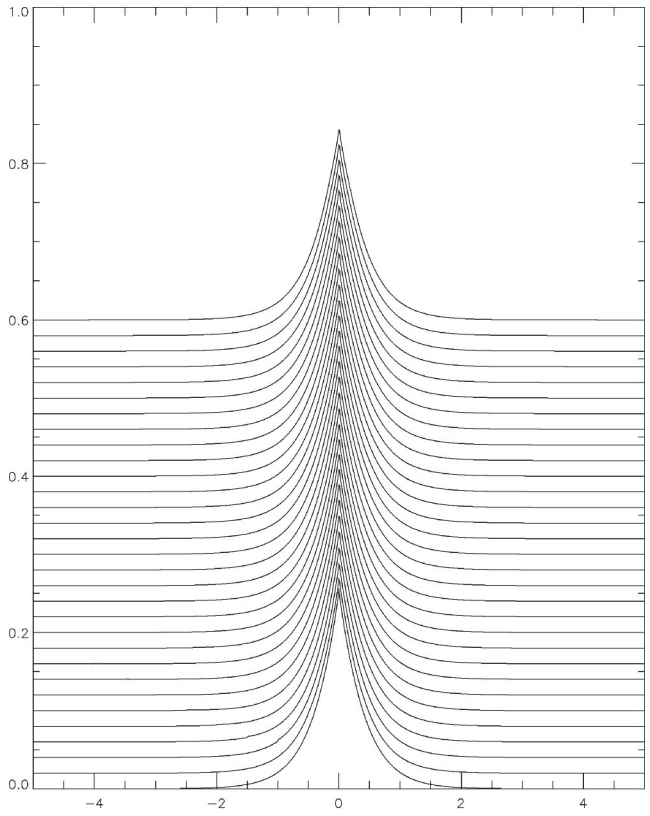

FIG. 7. An example of a stable peakon. The plot shows the field $|U_1|^2$ versus $x$ and $t$. The parameters are $\kappa=1.0$, $\alpha=1.95$, $\omega_0=1.5$, and $\omega=0.5$, with $\rho_0=0.04875$.

It was shown analytically above that Eqs. (17) and (18) (with $\sigma_3=0$) support peakons when $\rho_0>0$ and $\rho_0\kappa^2$ is very small. Direct simulations show that peakons do exist in this case, and they may be either unstable or stable. In the case when they are unstable, a high-wave-number instability develops around the central peak. In Fig. 7, we display the time evolution of a typical stable peakon.

Next, we look at what happens if we take a regular soliton as an initial condition in a section of the parameter space which supports only stable peakons. This enables us to study the competition of the structural stability of regular solitons (as confirmed in Fig. 6) and the stability of peakons. The initial condition is taken as a stationary regular soliton in the parameter region (close to the boundary of the peakon region) with $\rho_0<0$, whereas the simulations are run for values of the parameters corresponding to $\rho_0>0$, which only admits peakons and excludes regular solitons. Unlike the case shown in Fig. 6, the time evolution now does not exhibit internal vibrations. Instead, the pulse slowly decays into radiation. This outcome can be explained by the fact that the peakon's norm [see Eq. (8)] turns out to be larger than that of the initial pulse in this case, hence, its rearrangement into a stable peakon is not possible. An essential result revealed by the simulations is that cuspons may also be *stable*, a typical example being displayed in Fig. 8. In this figure, one can see a small shock wave which is initially generated at the cuspon's crest. It seems plausible that this shock wave is generated by some initial perturbation which could be a result of

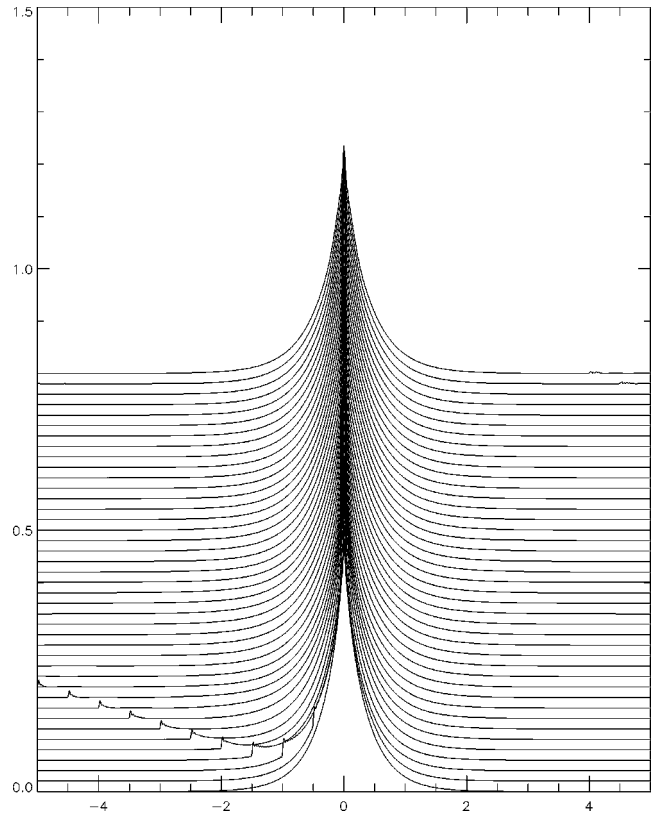

FIG. 8. An example of a stable cuspon. The plot shows the field $|U_1|^2$ versus $x$ and $t$. The parameters are $\kappa=1.0$, $\alpha=1.0$, $\omega_0=1.5$, and $\omega=0.5$, with $\rho_0=0.5$.

the finite mesh size in the finite-difference numerical scheme employed for the simulations. In fact, the emission of a small-amplitude shock wave is quite a typical way of the relaxation of both cuspons and peakons to a final stable state. To make sure that the shock wave is not an artifact generated by the numerical scheme, we have checked that its shape does not change with the increase of the numerical accuracy.

To further test the stability of the cuspons and peakons, in many cases we allowed the initially generated shock wave to reenter the integration domain (due to periodic boundary conditions used in the simulations) and interact again with the cuspon or peakon. As a result, the stability of the solitons of these types has been additionally confirmed. An example of the spatial profile of the cuspon established after a long evolution is shown in Fig. 9. Both the stability of the cuspon, and the presence of a tiny shock wave are evident in the figure.

However, unlike the regular solitons, which were found to be always stable, the cuspons are sometimes unstable. Typically, their instability triggers the onset of spatiotemporal collapse, i.e., formation of a singularity in a finite time (see a discussion of the feasible collapse in systems of the present type, given in the Introduction). Simulations of the collapse were possible with the use of an adaptive grid. A typical example of the collapse is shown in Fig. 10, where the inset shows that (within the numerical accuracy available) the amplitude of the collapsing pulse indeed diverges in a finite time.

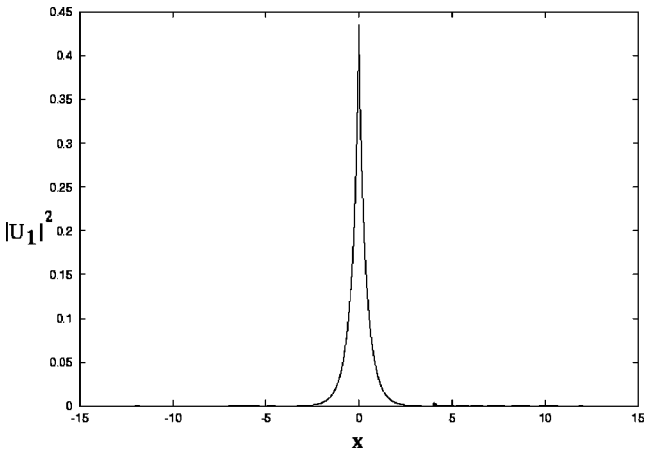

FIG. 9. The spatial profile of the stable cuspon at $t=20$. The parameters are the same as in Fig. 8.

However, the collapse is not the only possible outcome of the instability. In some other cases, which are not displayed here, the instability of peakons could be quite weak, giving rise to their rearrangement into regular solitons by the shedding of a small amount of radiation.

### C. Case $\sigma_3 \neq 0$

The predictions of the analysis developed above for the most general case, when the SPM terms are present in the model ($\sigma_3 \neq 0$), were also checked against direct simulations. As a result, we have found, in accord with the predictions, that only regular solitons exist in the case $\sigma_3 > 0$, while in the case $\sigma_3 < 0$, both regular solitons and peakons have been found as generic solutions. Further simulations, details of which are not shown here, demonstrate that both regular solitons *and* peakons are stable in this case.

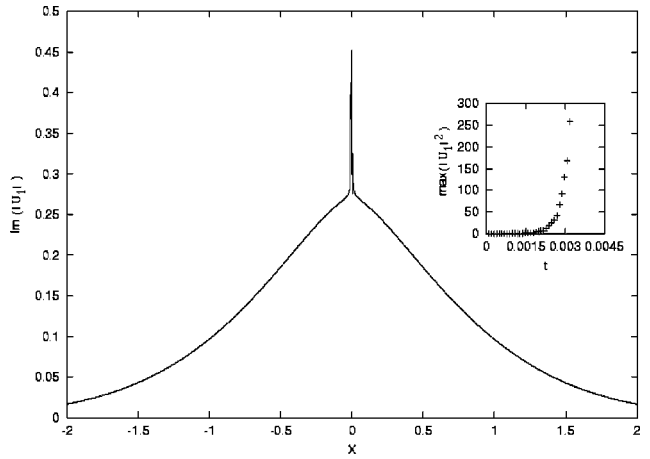

FIG. 10. The spatial profile is shown for an unstable cuspon in terms of $\mathrm{Im}\, U_1$ at $t=10^{-3}$. The inset depicts the time evolution of the maximum value of $|U_1|^2$. The transition to collapse is clearly seen as an explosive temporal behavior of the amplitude. The parameters are $\kappa=0.01$, $\alpha=1.1$, $\omega_0=0.1$, and $\omega=-0.3$, with $\rho_0=2.618$.

## IV. CONCLUSION

In this paper, we have introduced a generic model of three waves coupled by linear and nonlinear terms, which describes a situation when three dispersion curves are close to an intersection at one point. The model was cast into the form of a system of two waves with opposite group velocities that, by itself, gives rise to the usual gap solitons, which is further coupled to a third wave with zero group velocity (in the laboratory reference frame). Situations of this type are quite generic, being realizable in various models of nonlinear optics, density-stratified fluid flows, and in other physical contexts. In particular, two versions (temporal and spatial) of a nonlinear-optical model, which is based on a waveguide carrying the triple spatial Bragg grating, have been elaborated on in the Introduction. Our consideration was focused on zero-velocity solitons. In a special case when the self-phase modulation (SPM) is absent in the equation for the third wave, soliton solutions were found in an exact form. It was shown that there are two coexisting generic families of solitons: regular solitons and cuspons. In the special case when the coefficient of the linear coupling between the first two waves and the third one vanishes, cuspons are replaced by peakons. Direct simulations have demonstrated that the regular solitons are stable (in the case when the regular soliton is close to the border of the cuspon region, it has a persistent internal mode). The cuspons and peakons may be both stable and unstable. If they are unstable, they either shed off some radiation and rearrange themselves into regular solitons, or, in most typical cases, the development of the cuspon's instability initiates onset of spatiotemporal collapse. Actually, the present system gives the first explicit example of collapse in one-dimensional gap-soliton models.

The most general version of the model, which includes the SPM term in the equation for the third wave, has also been considered. Analysis shows that cuspons cannot exist in this case, i.e., cuspons, although being possibly dynamically stable, are structurally unstable. However, depending on the signs of the SPM coefficient, and some combination of the system's parameters, it was shown that a generic family of peakon solutions may exist instead. In accord with this prediction, the peakons have been found in direct simulations. The peakons, as well as the regular solitons, are stable in the system including the SPM term. We stress that peakons are physical solutions, as they have all their field components and their first derivatives finite.

The next step in the study of this system should be consideration of moving solitons, which is suggested by the well-known fact that the usual two-wave model gives rise to moving gap solitons too [1]. However, in contrast to the two-wave system, one may expect a drastic difference between the zero velocity and moving solitons in the present three-wave model. This is due to the reappearance of a derivative term in Eq. (6), when it is written for a moving soliton, hence, solitons which assume a singularity or jump in the $U_3$ component, i.e., both cuspons and peakons, cannot then exist. Nevertheless, one may expect that slowly moving solitons will have approximately the same form as the cuspons and peakons, with the singularity at the central point replaced by a narrow transient layer with a large gradient of the $U_3$ field. Detailed analysis of the moving solitons is, however, beyond the scope of this paper.

## ACKNOWLEDGMENTS

We would like to thank Tom Bridges, Gianne Derks, and Sebastian Reich for valuable discussions. B.A.M. and G.A.G. appreciate the hospitality of the University of Loughborough (UK). The work of G.A.G. is supported by a European Commission Grant, Contract No. HPRN-CT-2000-00113, for the Research Training Network *Mechanics and Symmetry in Europe* (MASIE).

[1] C. M. de Sterke and J. E. Sipe, in *Progress in Optics*, edited by E. Wolf (Elsevier, Amsterdam, 1994), Vol. XXXIII, Chap. 3, p. 205; A. B. Aceves, Chaos **10**, 584 (2000).

[2] G. Kurizki, A. E. Kozhekin, T. Opatrný, and B. A. Malomed, in *Progress in Optics*, edited by E. Wolf (Elsevier, Amsterdam, 2001), Vol. 42, Chap. 2, p. 93.

[3] R. Grimshaw, J. He, and B. A. Malomed, Physica D **113**, 26 (1998).

[4] D. N. Christodoulides and R. I. Joseph, Phys. Rev. Lett. **62**, 1746 (1989); A. Aceves and S. Wabnitz, Phys. Lett. A **141**, 37 (1989).

[5] N. G. R. Broderick, D. J. Richardson, R. I. Laming, and M. Ibsen, Opt. Lett. **23**, 328 (1998).

[6] B. J. Eggleton, R. E. Slusher, C. M. de Sterke, P. A. Krug, and J. E. Sipe, Phys. Rev. Lett. **76**, 1627 (1996); C. M. de Sterke, B. J. Eggleton, and P. A. Krug, J. Lightwave Technol. **15**, 1494 (1997).

[7] R. Grimshaw and B. A. Malomed, Phys. Rev. Lett. **72**, 949 (1994).

[8] J. Gear and R. Grimshaw, Stud. Appl. Math. **70**, 235 (1984).

[9] B. J. Eggleton, A. K. Ahuja, K. S. Feder, C. Headley, C. Kerbage, M. D. Mermelstein, J. A. Rogers, P. Steinvurzel, P. S. Westbrook, and R. S. Windeler, IEEE J. Sel. Top. Quantum Electron. **7**, 409 (2001); see, also, Opt. Express **9**, 675 (2001).

[10] D. G. Salinas, C. M. de Sterke, and J. E. Sipe, Opt. Commun. **11**, 105 (1994); C. M. de Sterke, D. G. Salinas, and J. E. Sipe, Phys. Rev. E **54**, 1969 (1996).

[11] W. C. K. Mak, B. A. Malomed, and P. L. Chu, Phys. Rev. E **58**, 6708 (1998).

[12] R. Grimshaw and B. A. Malomed, Phys. Lett. A **198**, 205 (1995).

[13] R. Camassa and D. D. Holm, Phys. Rev. Lett. **71**, 1661 (1993).

[14] R. A. Kraenkel and A. Zenchuk, J. Phys. A **32**, 4733 (1999); M. C. Ferreira, R. A. Kraenkel, and A. I. Zenchuk, *ibid.* **32**, 8665 (1999).

[15] A. S. Fokas and B. Fuchssteiner, Physica D **4**, 47 (1981).

[16] R. Beals and D. H. Sattinger, Inverse Probl. **15**, L1 (1999).

[17] T. Qian and M. Tang, Chaos, Solitons Fractals **12**, 1347 (2001).

[18] N. G. R. Broderick and C. M. de Sterke, Phys. Rev. E **58**, 7941 (1998).

[19] I. V. Barashenkov, D. E. Pelinovsky, and E. V. Zemlyanaya, Phys. Rev. Lett. **80**, 5117 (1998); A. De Rossi, C. Conti, and S. Trillo, *ibid.* **81**, 85 (1998).
[20] L. Bergé, Phys. Rep. **303**, 259 (1998).
[21] H. S. Eisenberg, R. Morandotti, Y. Silberberg, S. Bar-Ad, D. Ross, and J. S. Aitchison, Phys. Rev. Lett. **87**, 043902 (2001).
[22] A. R. Champneys, B. A. Malomed, and M. J. Friedman, Phys. Rev. Lett. **80**, 4169 (1998).